POLISH POLAR RESEARCH
vol. 46 no. 2, pp. 65–77 DOI: 10.24425/ppr.2025.154564

Anisotropy of magnetic susceptibility of Cretaceous to Eocene volcanic rocks from southern part of King George Island, West Antarctica

Jerzy NAWROCKI[1]* and Tomasz WERNER[2]

[1] *Polish Geological Institute – National Research Institute, Rakowiecka 4, 00-975 Warsaw, Poland*

[2] *Institute of Geophysics Polish Academy of Sciences, Księcia Janusza 64, 01-452 Warsaw, Poland*

***corresponding author:** *jerzy.nawrocki@pgi.gov.pl*

Received 28 November 2024 **Accepted** 27 May 2025

Abstract: The anisotropy of magnetic susceptibility (AMS) was determined for 147 specimens from 14 sites of Cretaceous to Eocene volcanics from south-central King George Island. For selected specimens parameters of hysteresis and thermomagnetic behavior were also studied. The AMS record was generally not modified by tectonic stress and deformations. In these weakly anisotropic rocks, the maximum susceptibility axes in most cases are convergent with the magma flow directions. The AMS data from the rocks cropping out close to the Ezcurra Fault do not support thesis about large scale dextral tectonic transport along it. The terrane model of this part of King George Island also seems to lack justification. The Ezcurra Fault most probably did not act as the strike-slip fault at least since the late Eocene.

Keywords: Antarctic, South Shetland Islands, magnetic anisotropy, lava flows.

Introduction

Anisotropy of magnetic susceptibility (AMS) is often used for the determination of directions of sedimentary transport and tectonic stress. Among other possibilities it can serve as a proxy for lava flow directions being derived from the viscous flow during its emplacement (Tauxe *et al.* 1998). The axis of maximum susceptibility (K_{max}) defines the magnetic lineation and K_{max} – K_{int} (intermediate axis), showing the magnetic foliation plane that is perpendicular to the minimum susceptibility axis K_{min} (Hrouda 1982). The most common feature is that samples with normal fabric have the K_{max} axes parallel to the flow plane (Knight and Walker 1988; Shi *et al.* 2003). The magnetic fabric imbrication along dyke margins and lava flows can help to determine sense of magma flow (Knight and Walker 1988; Aubourg *et al.* 2008; Simón-Muzás *at al.* 2022). Lava flows have fabrics that tend to be more foliated than lineated (Zananiri and Kondopoulou 2004). A flow-induced fabric can be overprinted by secondary processes such as tectonic stresses (Ellwood 1978) providing information about their directions (Borradaile and Henry 1997). Magnetic mineralogy strongly affects the AMS variation in volcanic rocks, providing scattered fabrics when late Ti-rich titanomagnetites dominate, and inverse or intermediate fabrics when single-domain grains are present (Moncinhatto *et al.* 2020). Generally, the application of AMS in lava flows is more complicated than in dykes and sills because the magma flows migrate in an open space and their upper margin does not provide imbricated fabrics that are important for directional information. Magnetic fabrics can define not only flow direction in particular site but can also be useful for determination of magma centers (MacDonald and Palmer 1990).

The Eocene to Oligocene is the time period with the strongest volcanic activity at King George Island (KGI), particularly common in its central part where volcanic rocks predominate (Nawrocki *et al.* 2010, 2011; Smellie *et al.* 2021a, 2021b). These sequences were studied paleomagnetically (Nawrocki *et al.* 2010, 2011; Gao *et al.* 2018) but have not been recognized in terms of application of the AMS yet.

The aim of this work is to define the nature of AMS of volcanic rocks from the central-southern part of KGI. Especially, we would like to answer the question if they recorded tectonic stress and their evolution in time. In the

case when the AMS would display the directions of magma flow only, the possible directions to the coeval igneous centers will be suggested.

Geological setting

The South Shetland Islands, located at the northwest of the Antarctic Peninsula are dominated by volcanic and plutonic rocks, with subsidiary areas of fore-arc and intra-arc sedimentary rocks (Smellie *et al.* 1984; Smellie 2021; Bastias *et al.* 2023). The South Shetland Island arc was formed during subduction of the Phoenix Plate under the Antarctic Plate between the latest Jurassic and the middle Miocene (Pankhurst and Smellie 1983; Willan and Kelley 1999; Smellie 2021). The archipelago was separated from the Antarctic Peninsula by the Bransfield Strait as a result of tectonic extensional processes in the Pliocene (Barker 1982; Barker and Dalziel 1983; Pańczyk and Nawrocki 2011). Earlier tectonic processes leading to the breakup of Patagonia from Antarctic Peninsula have been interpreted to occur between 50 and 30 Ma (Barker and Burrell 1977; Eagles and Jokat 2014).

KGI is located at the southern margin of the South Scotia Ridge and is the biggest island of the South Shetland Islands (Fig. 1A). It was subdivided (Birkenmajer 1983) into four major tectonic units separated by longitudinal strike-slip faults: the axial Barton Horst, the northern Fildes Block, the southern Warszawa Block and the southernmost Kraków Block (Fig. 1B). The Barton Horst is bounded in the south by the right-lateral strike-slip Ezcura Fault (Birkenmajer 2003) (Fig. 1C). A system of other strike-slip faults, transverse to the longitudinal faults, was subsequently used by Late Oligocene to Miocene dyke intrusions of the Admiralty Bay Group (Birkenmajer 1983; Pańczyk *et al.* 2009). The deep nature of the Ezcura Fault was documented by the seismic experiment (Majdański *et al.* 2008). A period of tectonic deformation close to the Miocene and Pliocene boundary post-dates the Cenozoic lava flows of KGI. According to Birkenmajer (1983) it was responsible for gentle folding of older volcanic rocks and for the formation of the Ezcura Fault.

The stratiform volcanogenic sequences of KGI are either monoclinal or arranged in gentle domes. In many places angular unconformities are observed between particular formations and even inside them. An unconformity of about 25º between the lavas of two formations was noted at Dufayel Island (Birkenmajer 2003). In most cases, it is not easy to distinguish if these angular unconformities are of tectonic origin or they result from a certain change of magma source location. For example, the results of palaeomagnetic studies of two sets of lava flows near the Italian Valley (Figs. 1C and 2A), inclined at different degree, indicate the depositional origin of the dip (Nawrocki *et al.* 2010).

It should be stressed that tectonic evolution of KGI has been only generally recognized and documented. Tokarski (1987) stated that brittle deformation prevails in the Late Mesozoic through recent volcanic sequence of KGI and on map scale shear deformation (strike-slip faults) prevails over extensional deformation with dykes. The geodynamic history of KGI was also studied by Kraus *et al.* (2010). The authors concluded that pronounced peak of intrusive activity was at 47–45 Ma and coincides well with a dramatic change in subduction zone parameters that caused a change from a compressional to an extensional tectonic regime.

Studied outcrops

During four field expeditions (2007, 2009, 2019 and 2022), 14 locations were visited with total of 33 hand and 51 drill samples collected for AMS and palaeomagnetic studies (Table 1). More than ten specimens were collected from six locations. From this reason our study can be treated as of a reconnaissance only.

Late Cretaceous lava flows

Uchatka Point

The Uchatka Point Formation consists of basalt lava flows 4–10 m thick cropping out south of the Paradise Cove (Figs. 1C, 2D and Birkenmajer 2003). At least 50 m of basalts sequence are covered by sedimentary rocks of the Creeping Slope Formation that gently incline to the NW (Birkenmajer 2002) at *ca.* 10º. A Late Cretaceous $^{40}Ar/^{39}Ar$ age (75.4 ± 0.9 Ma) was obtained from the bottom part of the section (Nawrocki *et al.* 2010). A set of 15 drill UP samples was taken from three lava flows of the middle part of the sequence that dips here at *ca.* 5º to the SE.

Paleocene lava flows

Keller Peninsula

The Keller Peninsula Formation was recognized and distinguished (Birkenmajer 2003) in the southern part of the Keller Peninsula. It consists of basaltic-andesite to andesite lavas, agglomerates and tuff. Two hand samples KL3 and KL4 were taken from the basaltic-andesite lava flows *ca.* 3–4 m thick dipping 5º to the NW and 15º to the NE, respectively. The $^{40}Ar/^{39}Ar$ isotope age of 60.6 ± 0.74 Ma was defined for the andesite sample near the Plaza Point where sample KL3 was taken (Nawrocki *et al.* 2021).

Earliest Eocene lava flows

Demay Point

The Demay Point Formation (Figs. 1C and 2C) consists of porphyritic dacite plug and extrusion (Birkenmajer 2003). In the outcrops near the Paradise Cove (Fig. 1C) the lava flows dip at *ca.* 15º to the SSE (near seashore) and *ca.* 10º to the NNW, *ca.* 300 m north from the seashore. They were dated by the $^{238}U/^{206}Pb$ method at 51.6 ± 0.8 Ma. On the classification diagram of Winchester and Floyd plot, they occupy trachyandesites field (Nawrocki *et al.* 2010). From three lava flows stretching out 30–150 m from the seashore, 26 drill DF samples were collected.

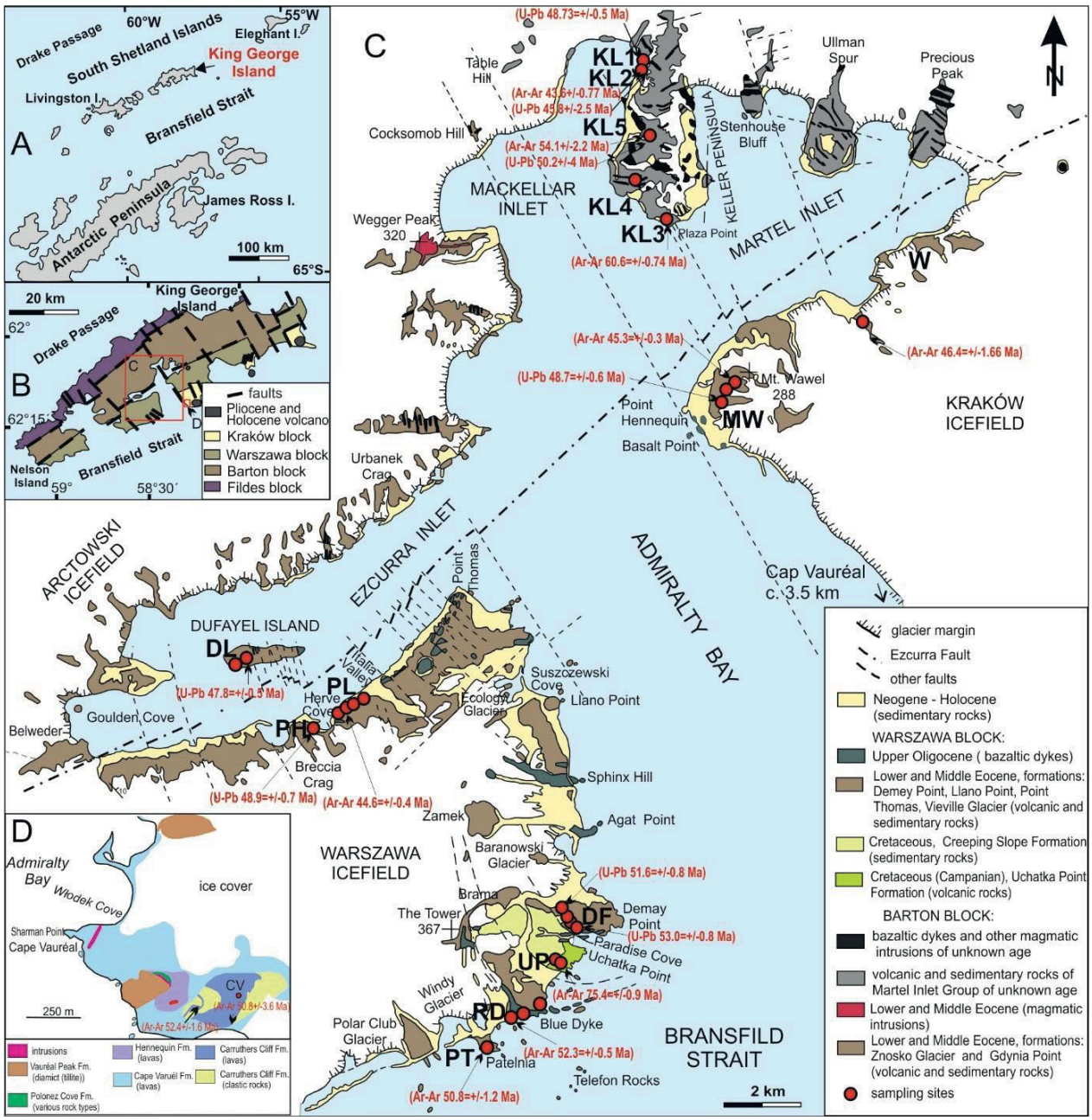

Fig. 1. The location of the studied area on King George Island on South Shetland Islands (**A**) and studied area overlain by structural units of King George Island (**B**) after Birkenmajer (1983), sites of the anisotropy of magnetic susceptibility studies (see text) on the background of simplified geological map of the central part of King George Island (**C**) after Birkenmajer (2003) and simplified geological map of Cap Vauréal area (**D**) after Smellie *et al.* (2021a). Isotope ages of studied rocks are also presented after Nawrocki *et al.* (2010, 2011, 2021) and Smellie *et al.* (2021a).

Blue Dyke Zone and Patelnia

The basaltic andesite lavas of the Llano Point Formation (Birkenmajer 2003), yielding at studied outcrops the $^{40}Ar/^{39}Ar$ ages of 52.3 ± 0.5 Ma and 50.8 Ma (Nawrocki *et al.* 2010), were sampled (samples RD1, RD2 and RD3) in the vicinity of younger vertical intrusion, the Blue Dyke (Pańczyk *et al*. 2009). Additionally, two hand samples (PT1 and PT2) were taken from the massive, dark grey lava flows of this formation on the Patelnia Peninsula (Figs. 1C and 2E). Near the Blue Dyke the lava flows tilt at *ca.* 20º to the south and on the Patelnia Peninsula at *ca.* 10º to the SW.

Keller Peninsula

One hand sample (KL5) was taken from the andesite lava flow of the Visca Anchorage Formation cropping out in the middle part of the Keller Peninsula and dated here at 50.2 ± 4 Ma (Nawrocki *et al*. 2021). It dips at *ca.* 5º to the NW.

Kap Vaureal

The Carruthers Cliff Formation (Fig. 1D) is of Eocene age of 52.4–50.8 Ma by $^{40}Ar/Ar^{39}$ (Smellie *et al.* 2021a). One hand sample (CV1) was taken from the andesite lava flow of this formation dipping at *ca.* 25º towards the WSW.

Table 1. Volcanogenic rocks from central part of King George Island sampled for the anisotropy of magnetic susceptibility study.

Site	Symbol	Rock type	Sample type and number	Number of specimens	Isotopic age
Late Cretacous lava flows					
Uchatka Point	UP	basalt	15 drill samples	15	75.4+/-0.9 Ma
Palaeocene lava flows					
Keller Penninsula	KL (3, 4)	basalt-andesite	2 hand samples	6	60.6+/-0.74 Ma
Earliest Eocene lava flows					
Demay Point	DF	porphyritic dacite	20 drill +6 hand samples	36	51.6+/-0.8Ma
Blue Dyke Zone and Patelnia	RD, PT	basalt-andesite	3 hand samples (RD), 2 hand samples PT	9	52.3+/-0.5Ma
Keller Penninsula	KL (5)	andesite	1 hand sample	2	50.2+/-4Ma
Kap Vaureal	CV	basalt	1 hand sample	5	52.4+/-1.6Ma, 50.8+/-3.8Ma
Late Early to Middle Eocene					
Italian Valey	PL	basaltic	16 drill samples	16	44.9+/-0.7Ma; 44.6+/-0.4Ma
Herve Cove	PH	basaltic trachyadesite	2 hand samples	4	48.9+/-0.5Ma
Dufayel Island	DL	basaltic trachyadesite	3 hand samples	13	47.8+/-0.5Ma
Mount Wawel	MW	andesite	9 hand samples, 2 units	16	48.7+/-0.6Ma; 45.3+/-0.3Ma
Keller Penninsula	KL (1, 2)	andesite	2 hand samples	6	48.73+/-45.8Ma
Warkocz	W	andesite	2 samples	6	46.4+/-1.66Ma

Late Early to Middle Eocene lava flows

Italian Valley – Herve Cove

The basaltic rocks of the Point Thomas Formation exposed along the southern coast of Ezcura Inlet were sampled in two sections. The section extending from the Italian Valley along the Dutkiewicz Cliff (16 drill PL samples) provided $^{40}Ar/^{39}Ar$ isotope ages of 44.9 ± 0.7 Ma and 44.6 ± 0.4 Ma (Nawrocki *et al*. 2010). The lava flows (Fig. 2A) are inclined here at *ca.* 20º towards the SW in eastern part of the section and at *ca.* 38º to the south in its western part. The basaltic trachyandesites from the Herve Cove dip at *ca.* 20º to SSW. Three hand samples (PH) were taken from three lava flows dated at 48.9 ± 0.5 Ma with the $^{238}U/^{206}Pb$ method (Nawrocki *et al.* 2011).

Dufayel Island

Three hand DL samples of weakly altered rocks of the Znosko Glacier Formation cropping out at Dufayel Island were taken. These rocks, dated at 47.8 ± 0.5 ($^{238}U/^{206}Pb$ method) on the classification diagram of Winchester and Floyd fall within the basaltic trachyandesite and trachyandesite fields (Nawrocki *et al.* 2010). The lava flows sampled are inclined at *ca.* 15º towards the west.

Mount Wawel

Two geological units, the Vieville Glacier and Mount Wawel Formations (Birkenmajer 2003) redefined and incorporated into one unit the Hennequin Formation by Smellie *et al.* (2021a) were sampled on the southern slope of the Mount Wawel (Fig. 2F). They consist of andesite lava flows (Birkenmajer 2003) dated at 48.7 ± 0.6 Ma and 45.3 ± 0.3 Ma with the $^{238}U/^{206}Pb$ and $^{40}Ar/^{39}Ar$ methods, respectively (Nawrocki *et al.* 2011). The lava flows are inclined at *ca.* 15º to the NE. Nine hand MW samples were taken for the AMS study.

Keller Peninsula

Two hand samples (KL1 and KL2) were taken from the andesites of Domeyko Glacier Formation. This formation was dated to be 48.73 to 45.8 Ma old, according to the

Fig. 2. Photo panoramas of the studied sections: (**A**) Italian Valley in Herve Cove, (**B**) Dufayel Island, (**C**) Demay Point, (**D**) Uchatka Point, (**E**) Patelnia Peninsula and (**F**) Mount Wawel. Sampling sites/locations are indicated.

$^{238}U/^{206}Pb$ method (Nawrocki *et al.* 2021). The sampled lava flows are inclined at *ca.* 5–10º towards the NW.

Warkocz

The Warkocz sequence cropping out east of the Wanda Glacier consists of ignimbrites, conglomerates and andesite lava flows on the top (Smellie *et al.* 2021a). The $^{40}Ar/^{39}Ar$ isotope age indicates its Middle Eocene 46.4 ± 1.66 Ma and 49.4 ± 8.4 Ma ages (Smellie *et al.* 2021a). H and samples W1 and W2 were taken from the andesite lava flow that dips at 12º towards the NE.

Methods

The drill and hand samples were cut into 147 cylindrical (25 mm in diameter and 22 mm in length) specimens. The magnetic susceptibility and its anisotropy were measured by means of a KLY3 kappabridge (Agico, Czechia) at Laboratory for Paleomagnetism and Environmental Studies at Institute of Geophysics Polish Academy of Sciences (IGF PAS) and MFK1-FB kappabridge (Agico, Czechia) at Polish Geological Institute - NRI. The AMS parameters (Jelinek 1981) were computed using the ANISOFT software. The 95% confidence uncertainty ellipses were determined using the linear perturbation analysis described by Jelinek (1978). The semi axis of the uncertainty ellipse e was labelled by number 1, 2 and 3 assigned to principal axes of anisotropy ellipsoid K_{max}, K_{int}, and K_{min}, respectively. Measurements with statistical parameters e12 < 22.5° and F12 > 4 were considered as recording a statistically significant magnetic lineation. A statistically significant magnetic foliation was in samples with e23 < 30° and F23 > 10 (Langroix and Banerjee 2004).

Parameters of hysteresis were obtained with AGM 2900-02 Micromag alternating gradient force magnetometer (Princeton Measurements Corporation, USA) at Laboratory for Paleomagnetism and Environmental Studies at IGF PAS. For selected samples changes of magnetic susceptibility were monitored with the KLY3 kappabridge with CS3 high temperature unit (Agico S.r.o., Czechia) at IGF PAS. Powdered samples were subsequently heated and cooled in the range of 20–700°C in air atmosphere. The SAFYR and CUREVAL software (Agico, Czechia) were used for data processing.

Results

Magnetic carriers

All magnetic susceptibility versus temperature curves are irreversible (Fig. 3A). Changes of magnetic susceptibility during subsequent heating indicate varying contribution of magnetic phases with Curie temperatures of about 500ºC (samples UP1, DF7), 580ºC (samples UP1, UP7, DF7), 620ºC (samples DF7, UP7). Ti-poor titanomagnetites, magnetite and may be hematite are present in studied samples. Most probably the secondary hematite was formed from the maghemite during subsequent heating of samples as can be inferred from the decrease of magnetic susceptibility at temperature of *ca.* 450ºC (samples UP1 and DF7). A significant drop of magnetic susceptibility noted on the cooling curve may be caused exactly by the oxidation of maghemite to hematite (Dunlop and Özdemir 1997).

A plot of coercivity of remanence (Hcr) versus coercivity (Hc), shows strict positive correlation of these parameters (Fig. 3B). On the plots presenting the ratio of saturation magnetization to saturation remanence (Mr/Ms) and the ratio of coercivity of remanence to coercivity (Hcr/Hc) (Dunlop 2002; Day *et al.* 2007), the samples cluster in the range characteristic for the mixture of single- and multidomain grains (Fig. 3C). On the Day-Dunlop plot with mixing curves (Dunlop and Carter-Stiglitz 2006), most of samples are grouped in the area indicative for the pseudo single domain grains (Fig. 3D). It should be stressed, however, that the reference curves were established for the pure magnetite. In the studied samples, apart from this mineral, the maghemite, Ti-poor titanomagnetite and most probably hematite occur.

Anisotropy of magnetic susceptibility

The lowest mean volume magnetic susceptibility (9.4–13.5 x 10^{-3} SI units) were measured in samples from the Dufayel Island (DL1–DL3), Keller Peninsula (KL2) and Warkocz (W1–W2). The highest mean value of this parameter (66.93 10^{-3} SI units) is characteristic for samples from Mount Wawel (Table 2). The studied samples are only weakly anisotropic with values of the corrected anisotropy factor Pj are up to 1.037 (Table 2). Highest mean value of Pj (1.052) was noted for the sample KL4 from the Keller Peninsula. The shape parameter T ranging from −0.503 to 0.579 indicate the occurence in particular localities of different, *i.e.*, the prolate, triaxal or oblate magnetic fabrics. There is no mutual relationship between the mentioned above three parameters (Fig. 4).

Samples with normal magnetic fabric

The foliation plane is gently imbricated and the lineation is close to the foliation plunge in late Cretaceous basalts from the Uchatka Point Formation (Fig. 4). Both fabrics elements regarded as a normal (Knight *et al.* 1986; LaBerge *et al.* 2009) determine the flow direction that is consistent with the direction of the lava stream dip. In the mid-Eocene volcanogenic succession from the Italian Valley section, the foliation plane is almost horizontal but the azimuth of the mean K_{min} axis is close to the direction of lineation. Because of error of the mean K_{min} determination greater than the angle of imbrication of this axis, the magnetic foliation's orientation is not sufficient factor to determine the flow direction (Agrò *et al.* 2015). The SSW-NNE direction of lineation is between the directions of the dip of lava flows forming the bottom and upper part of the Italian Valley sequence (Fig. 4). The anisotropy ellipsoids determined for both mentioned localities have a mixed shape. The normal magnetic fabric is also characteristic for the late Eocene volcanic rocks from Dufayel Island and Warkocz (Fig. 5). Also, two specimens of Paleocene lava from the Keller Peninsula (sample KL4) display the same normal magnetic fabric.

Samples with dipping magnetic foliation

In the Early Eocene Demay Point Formation the K_{max} axes are quite well clustered. The directions of the lava flows dip are convergent with them (Fig. 4). However, the K_{min} axes are stretched at the stereoplot with most of them strongly inclined to the west. The rocks display a very weak foliation and consequently predominantly prolate shape of the AMS ellipsoid.

The similar pattern of the AMS axes with dipping magnetic foliation can be observed in the lower part of the Mount Wawel section. Its upper part contains normal magnetic fabrics but with stretched K_{min} axes along the plane perpendicular to the direction of lava flows dip and K_{min} axes (Fig. 4).

In the early Eocene basaltic andesite lavas sampled near the younger vertical intrusion the Blue Dyke, the K_{min} axes are inclined easterly at *ca.* 40º. Most of K_{max} axes are in the opposite side of the hemisphere but the dip of lava flows is transverse to them (Fig. 5). The K_{min} axes determined for particular specimens of the Late Eocene andesite lava flow from the Keller Peninsula (sample KL1) are stretched in the plane perpendicular to the K_{min} axes that are consistent with the direction of lava flow dip. The AMS ellipsoid is here prolate with a very weak foliation (Fig. 5).

Samples with reverse and transverse magnetic fabric

Transverse magnetic fabric with K_{max} perpendicular to the magma flow direction and azimuth of K_{min} axes can be observed in the early Eocene basaltic andesite lava from the Patelnia Peninsula. This type of magnetic fabric with the lineation orthogonal to the foliation plunge is also characteristic for the Eocene andesite lava flow from the Cape

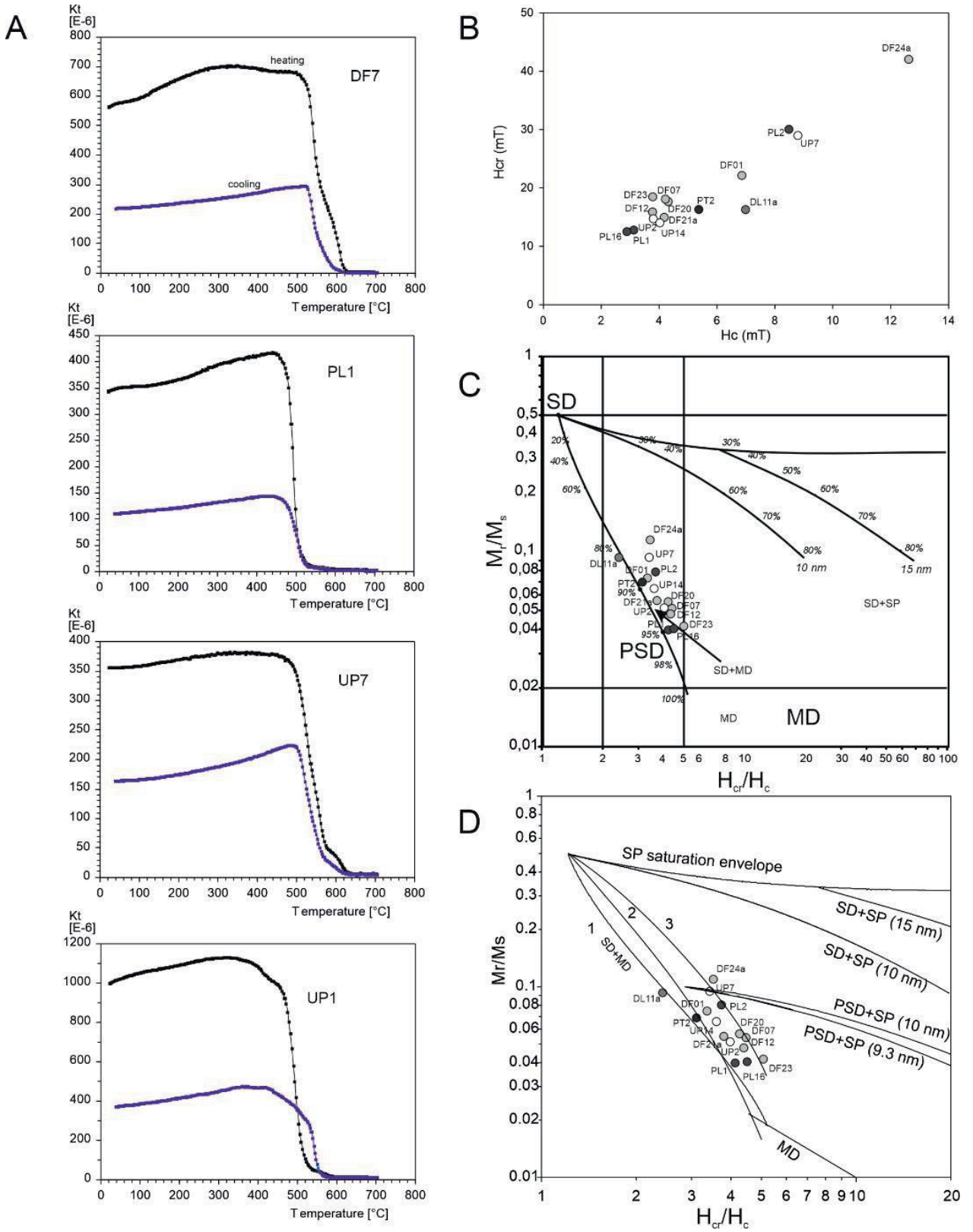

Fig. 3. (**A**) magnetic susceptibility (Kt) versus temperature curves determined for samples from Demay Formation (DF7), Point Thomas Formation in Italian Valley (PL1) an Uchatka Point Formation (UP1, UP7), (**B**) coercivity of remanence (Hcr) versus coercive force (Hc) plot, (**C**) day plot: ratio of saturation remanent magnetization to saturation magnetization (Mr/Ms) against the ratio of coercivity of remanence to coercive force (Hcr/Hc) for samples from Demay Formation (DF), Point Thomas Formation (PL), Uchatka Point Formation (UP) and Lano Point Formation at Patelnia Peninsula (PT). Single-domain (SD), pseudo-single domain (PSD) and multi-domain (MD) plot boundaries are taken from Dunlop (2002) and (**D**) hysteresis ratios for the same samples on the Day-Dunlop plot with mixing curves. Curves 1, 2 and 3 represent different mixing curves of single-domain and multi-domain magnetite after Dunlop (2002).

Table 2. Mean values of magnetic susceptibility (K. x 10^{-3} SI u.). corrected anisotropy factor (Pj) and shape parameter (T) calculated for particular localities on the King George Island (see Fig. 1). N – number of samples, n – number of specimens.

Locality	N/n	K_{mean}	Pj	T
DF	26/36	33.63	1.035	-0.416
DL	3/13	10.62	1.018	0.259
PH	3/4	53.51	1.022	0.139
PL	16/16	58.12	1.022	0.024
PT	2/4	58.51	1.023	0.008
RD	3/5	50.42	1.026	0.268
UP	15/15	54.78	1.034	0.094
MW	9/16	66.93	1.021	0.231
KL1	1/4	21.61	1.023	-0.503
KL2	1/2	9.44	1.037	-0.012
KL3	1/2	37.93	1.029	-0.185
KL4	1/4	47.75	1.052	0.143
KL5	1/2	36.08	1.031	0.195
W	2/6	13.53	1.017	0.579
CV	1/5	62.31	1.015	-0.272

Vaureal (Fig. 5). The reverse fabric, consisting of the exchange of the minimum and maximum anisotropy axes and commonly linked with the occurrence of single-domain magnetite (Rochette *et al.* 1999), was detected in two samples KL2 and KL3 of the Palaeocene andesite from the Keller Peninsula (Fig. 5). It should be stressed, however, that the AMS data were received from four specimens only.

Discussion

Azimuths of the dip of the lava flows, characteristic for the late Eocene sequence at Dufayel Island and in the Italian Valley section, are comparable with the lava flow directions inferred from the AMS data. Palaeomagnetic data from the Italian Valley volcanogenic sequence (Nawrocki *et al.* 2010) indicate the primary, *i.e.*, not disturbed by tectonic processes origin of its dip. Hence, one can conclude that volcanic center was located beyond the present-day land in the Ezcurra Inlet and the magma migration paths may be linked with the discontinuity of the Ezcurra Fault (Fig. 6). Birkenmajer (2003) interprets the Ezcurra Fault as right-lateral strike-slip with the motion that began at *ca.* 54 Ma and continued for a period of at least 33 Ma. If so, then crossing of the lava flow directions on the Ezcurra Fault line is rather accidental because the Dufayel Island and Italian Valley sequence are located in the opposite sides of this line. However, the most likely solution is that the Ezcura Fault did not act as the strike-slip with significant translation at least since the Late Eocene because the pattern of the AMS axes is generally not disturbed by the activity of this prominent discontinuity.

Basing on the AMS data, it is impossible to define unequivocally location of the magma center for the basaltic andesite lavas on the Patelnia Peninsula. The azimuths of K_{max} and K_{min} axes are not convergent with the azimuth of dip of magma flow in these rocks that are characterized by the transverse magnetic fabric. Only the axes of intermediate susceptibilities K_{int} are close to it (Fig. 5). Maybe it is related to fast transport of lava and the rolling of elongate grains. The same problem applies to the rocks with dipping magnetic foliation sampled in the Blue Dyke Zone where the AMS data do not correspond to the direction of dip of lava flows. Most probably, the tectonic processes related to emplacement of the younger Blue Dyke intrusion (27.9 ± 0.3 Ma; Pańczyk *et al.* 2009) changed the original dip of the lava flows and consequently inclined the K_{min} and K_{max} axes. The AMS axes and the dip of the lava flows characteristic for the Cretaceous basalts of the Uchatka Point Formation clearly indicate inland magmatic center located NW of the studied sites. The adjacent Demay Point Formation consisting of acid volcanic rocks has a complex nature. Apart from the lava flows, it consists of plugs, dykes and extrusions (Birkenmajer 2003). The inclined and stretched minimum susceptibility axes are likely related to this complicated environment of the magma emplacement. The K_{max} axes could indicate that the magmatic center for the studied flows was most probably located NNW of them.

Mount Wawel is presented by Birkenmajer (2003) as the remnant of the volcano with the lava flows inferred to dip into its center. The AMS data from the lower and upper parts of the Mount Wawel sequence display the SW-NE oriented lava flows but the directions of imbrication of K_{max} and K_{min} axes are opposite in both parts of the section, The location of magma center cannot be, however, inferred from this set of AMS data. Detailed studies of bottom and upper parts of particular lava flows are necessary. The azimuth of the dip of lava flows could indicate the magma center located SW of the studied sites. Part of the AMS data from the Keller Peninsula (samples KL1, KL3 and KL4), although of poor statistical representativeness, are convergent with the directions of magma flows dip and inland centers of magma that are shown by the location of K_{max} axes (Figs. 5 and 6).

Magnetic fabric may be substantially modified especially in the zones of ductile deformations of volcanic rocks (Hrouda and Chadima 2020). In slightly deformed volcanic rocks of KGI, where the brittle deformation prevails (Tokarski 1987), the magnetic fabric can be also modified in the sites located close to tectonic faults (Atarita *et al.* 2019). The pattern of the AMS axes in the studied sites is generally not disturbed by tectonic stress. The K_{max} axes in most cases

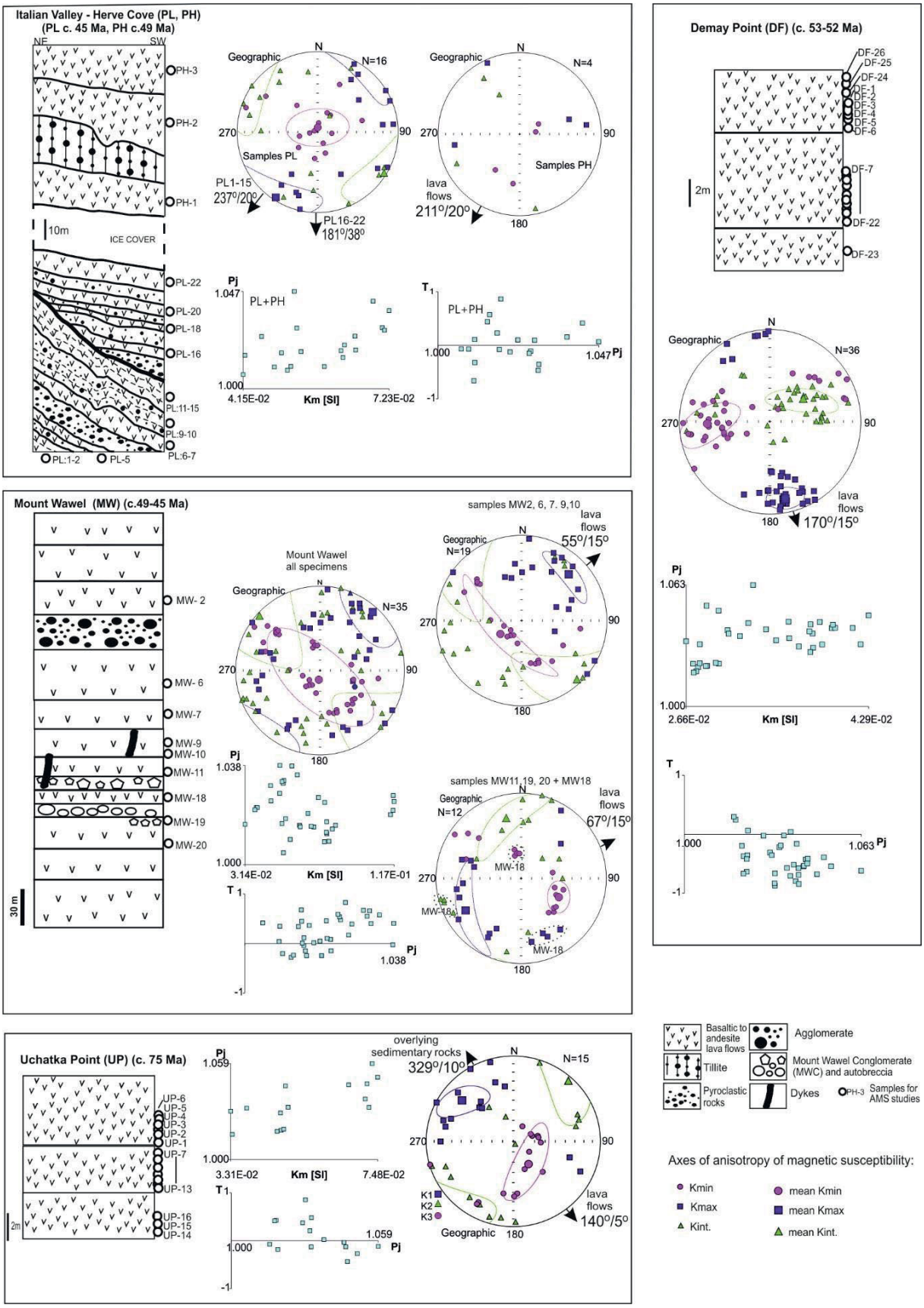

Fig. 4. Simplified lithological sections of studied volcanogenic rocks from Italian Valley – Herve Cove, Demay Point, Mount Wawel and Uchatka Point localities (with sampling sites marked), and stereographic projections (lower hemisphere) of AMS axes obtained from them. The graphs of corrected anisotropy parameter (Pj) versus magnetic susceptibility (Km) and shape parameter (T) versus corrected anisotropy parameter are also presented.

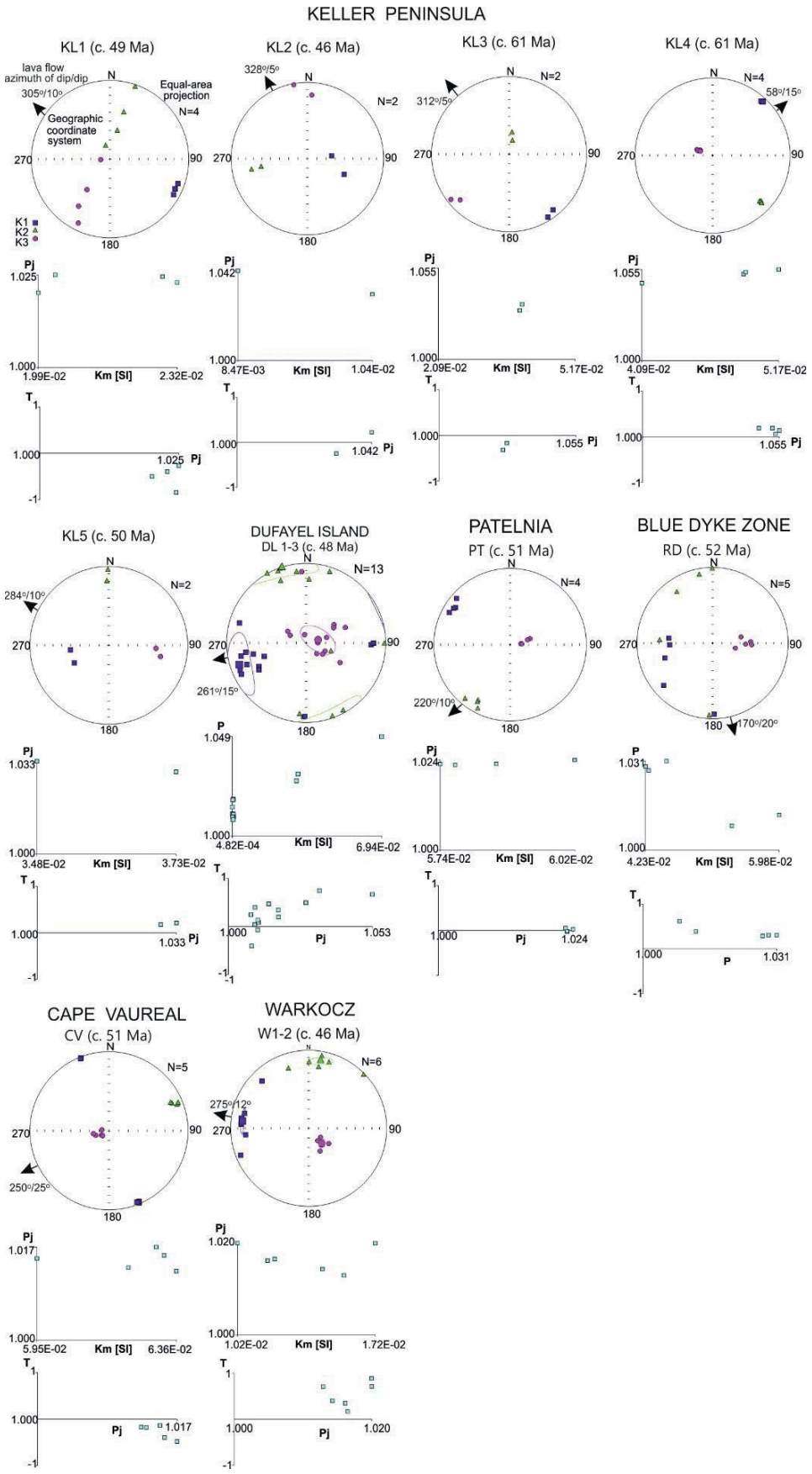

Fig. 5. Stereographic projections of AMS axes obtained from the Keller Peninsula, Dufayel Island, Patelnia, Blue Dyke Zone, Cape Varuel and Warkocz localities. The graphs of corrected anisotropy parameter (Pj) versus magnetic susceptibility (Km) and shape parameter (T) versus corrected anisotropy parameter are also presented. Symbols of AMS axes on stereonets as in Fig. 4.

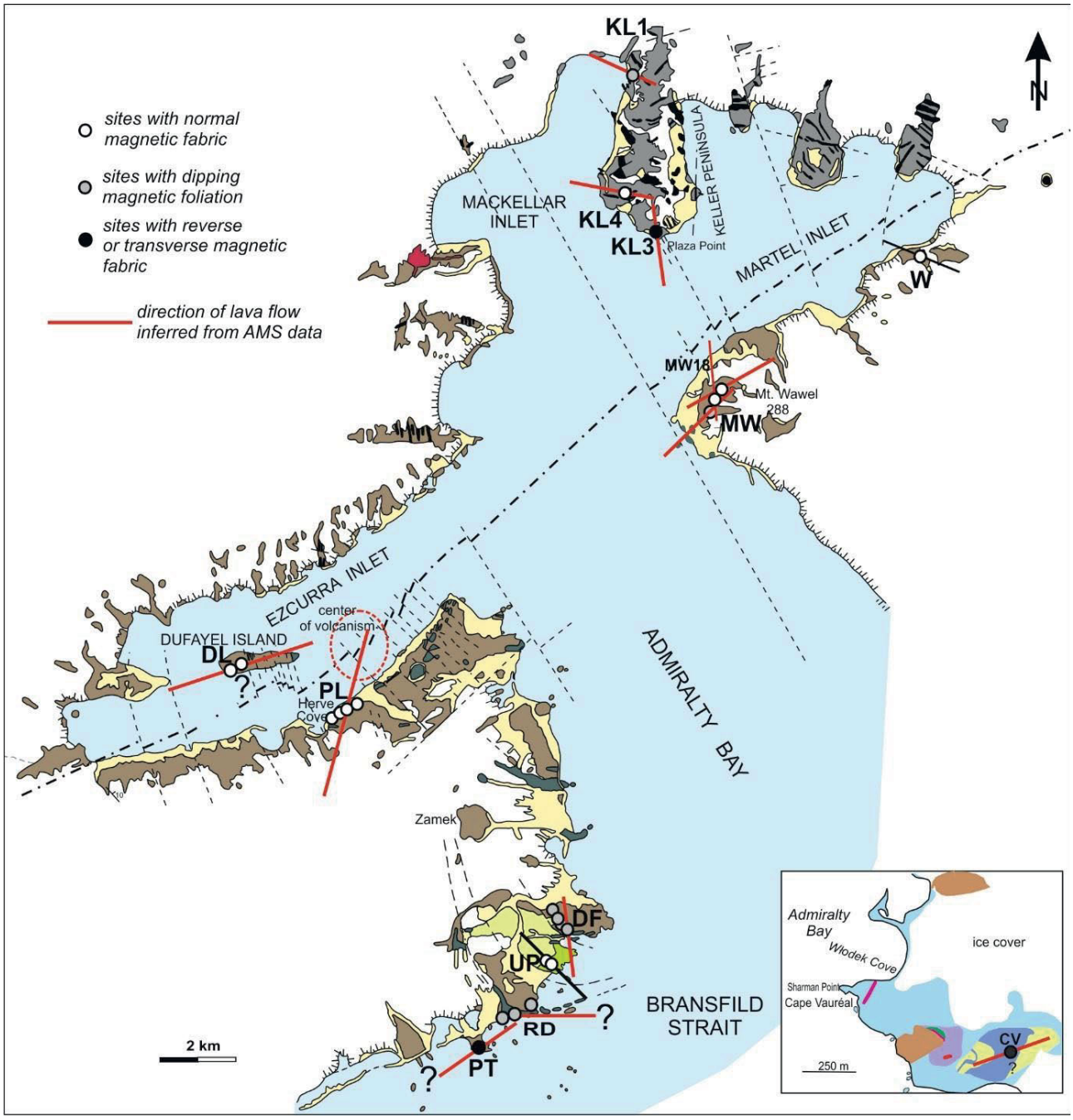

Fig. 6. Directions of flows for lavas in the studied localities as inferred from the anisotropy of magnetic susceptibility measurements. They are presented on the background of simplified geological map of central part of King George Island after Birkenmajer (2003) and simplified geological map of Cap Vauréal area after Smellie *et al.* (2021a), for explanations see Fig. 1. Types of magnetic fabric and dipping magnetic foliation are distinguished.

are convergent with the magma flow direction and the degree of anisotropy is relatively low. There are no traces of tectonic disturbance of the AMS record even in the sites located close to the Ezcurra Fault. Consequently, our data rather do not support the large scale dextral tectonic transport along the Ezcurra Fault and the terrane model of this part of KGI (Birkenmajer 2003). Most probably this prominent discontinuity was acted as a normal, not strike-slip type fault. Such an interpretation can be supported by the newest isotope ages of magmatic rocks. The comparison of stratigraphy of the Warszawa, Kraków, and Barton blocks presented by Birkenmajer (2002, 2003) with the newest U/Pb and $^{40}Ar/^{39}Ar$ ages has necessitated the substantial modification of the local stratigraphic chart (Nawrocki *et al.* 2010, 2011). The isotopic age estimates for selected igneous rocks allowed to distinguish common Cenozoic magmatic activity phases for all mentioned above tectonic units that were previously distinguished as separate events characteristic for particular tectonic unit only (Nawrocki *et al.* 2011; Smellie *et al.* 2021a, 2021b).

Conclusions

The AMS record in the Cretaceous to Eocene volcanic rocks is generally not disturbed by tectonics. The K_{max} axes in most cases are convergent with the magma flow direction and the degree of anisotropy is relatively low. The AMS data from the rocks located in the vicinity of the Ezcura Fault rather do not support the thesis about large scale dextral tectonic transport along this fault and the terrane model of this part of the KGI. The Ezcurra Fault most probably has not acted as the large strike-slip at least since the late Eocene. The volcanic center for the late Eocene magma flows of the Italian Valley and Dufayel Island sections was located beyond the present-day land in the Ezcurra Inlet. The magma migration path could be located in the discontinuity of the Ezcurra Fault.

Acknowledgments

The analytical research and field work was funded by the National Fund for Environmental Protection and Water Management (project No: 22.6014.1901.02.1). This study was also supported by a grant of the Polish Ministry of Science and Higher Education (No. N N307 058434). Magdalena Pańczyk, Krystian Wójcik, Agata Kozłowska-Roman, Ewelina Krzyżak, Rafał Małek and the logistics team of the Arctowski Polish Polar Station (Institute of Biochemistry and Biophysics PAS) are acknowledged for their support during field work. Rafał Szaniawski and John Smellie are warmly acknowledged for critical review of our manuscript.

References

Agrò A., Zanella E., Le Pennec J-L. and Temel A. 2015. Magnetic fabric of ignimbrites: a case study from the Central Anatolian Volcanic Province. *Geological Society London, Special Publications* 396: 159–175, doi: 10.1144/SP396.9.

Atarita F.R., Bijaksana S., Ndari N.R., Pratama A., Taqwantara R.F., Fajar S.J. and Latief F.D. 2019. Anisotropy of magnetic susceptibility and preferred pore orientation in lava flow from the Ijen Volcanic Complex, Eastern Java, Indonesia. *Geosciences* 9: 304, doi: 10.3390/geosciences9070304

Aubourg C., Tshoso G., LeGall B., Bertrand H., Tiercelin J.-J., Kampunzu A.B., Dyment J. and Modisi M. 2008. Magma flow revealed by magnetic fabric in the Okavango giant dyke swarm, Karoo igneous province, northern Botswana. *Journal of Volcanology and Geothermal Research* 170: 247–261.

Barker P.F. 1982. The Cenozoic subduction history of the Pacific margin of the Antarctic Peninsula: ridge crest-trench interactions. *Journal of Geological Society of London* 139: 787–801.

Barker P.F. and Burrell J.1977. The opening of Drake Passage. *Marine Geology* 25: 15–34.

Barker P.F. and Dalziel I.W.D. 1983. Progress in geodynamics in the Scotia Arc region. *In:* R. Cabre (ed.) Geodynamics of the Eastern Pacific Region, Caribbaen and Scotia Arcs. *Geodynamics series* 9: 137–170.

Bastias J., Chew D., Villanueva C., Riley T., Manfroi J., Trevisan C., Leppe M., Castillo P., Poblete F., Tetzner D., Giuliani G., Lopez B., Chen H., Zheng G-G., Zhao Y., Gao L., Rauch A. and Jana R. 2023. The South Shetland Islands, Antarctica: Lithostratigraphy and geological map. *Frontiers in Earth Science* 10: 1002760, doi: 10.3389/feart.2022.1002760.

Birkenmajer K. 1983. Late Cenozoic phases of block-faulting on King George Island (South Shetland Island, West Antarctica). *Bulletin Academie Polonaise des Sciences: Terre* 30: 21–32.

Birkenmajer K. 2002. Admiralty Bay, King George Island, South Shetland Islands, West Antarctica. *Geological map 1:50 000.*

Birkenmajer K. 2003. Admiralty Bay, King George Island (South Shetland Islands, West Antarctica): A geological monograph. *In:* Birkenmajer K. (ed.) *Geological results of the Polish Antarctic expeditions. Part XIV. Studia Geologica Polonica* 120: 1–75.

Borradaile G.J. and Henry B. 1997. Tectonic applications of magnetic susceptibility and its anisotropy. *Earth-Science Reviews* 42: 49–93.

Day R., Fuller M. and Schmidt V.A. 1977. Hysteresis properties of titanomagnetites: grain-size and compositional dependence. *Physics Earth and Planetary Interior* 13: 260–267.

Dunlop D.J. 2002. Theory and application of the Day plot (Mrs/Ms versus Hcr/Hc). 1. Theoretical curves and tests using titanomagnetite data. *Journal of Geophysical Research* 107: B3, doi: 10.1029/2001jb000486.

Dunlop D.J. and Özdemir Ö. 1997. Rock Magnetism Fundamentals and Frontiers. Cambridge University Press, New York, London and Cambridge.

Dunlop D.J. and Carter-Stiglitz B. 2006. Day plots of mixures of superparamagnetic, single-domain, pseudosingle-domain, and multidomain magnetites. *Journal of Geophysical Research* 111: B12S09, doi: 10.1029/2006jb004499.

Eagles G. and Jokat W. 2014. Tectonic reconstructions for paleobathymetry in Drake passage. *Tectonophysics* 611: 28–50.

Ellwood B.B. 1978. Flow and emplacement direction determined for selected basaltic bodies using magnetic susceptibility anisotropy measurements. *Earth and Planetary Science Letters* 41: 254–264, doi: 10.1016/0012-821X(78)90182-6.

Gao L., Zhao Y., Yang Z., Liu J., Liu X., Zhang S.H. and Pei J. 2018. New paleomagnetic and $^{40}Ar/^{39}Ar$ geochronological results from the South Shetland Islands, west Antarctica, and their tectonic implications. *Journal of Geophysical Research: Solid Earth* 123: 4–30, doi: 10.1002/2017JB014677.

Hrouda F. 1982. Magnetic anisotropy of rocks and its application in geology and geophysics. *Surveys in Geophysics* 5: 37–82.

Hrouda F. and Chadima M. 2020. Examples of tectonic overprints of magnetic fabrics in rocks of the Bohemian Massif and Western Carpathians. *International Journal of Earth Sciences* 109: 1321–1336, doi: 10.1007/s00531-019-01786-8.

Jelinek V. 1978. Statistical processing of magnetic susceptibility measured in groups of specimens. *Studia Geophysica et Geodethica* 22: 50-62.

Jelinek V. 1981. Characterization of magnetic fabrics of rocks. *Tectonophysics* 79: 63–67.

Knight M.D. and Valker G.P.L. 1988. Magma flow directions in dikes of the Koolau Complex, Oahu, determined from magnetic fabric studies. *Journal of Geophysical Research and Space Physics* 93: 4301–4319.

Knight M.D., Walker G.P.L., Elwood B.B. and Diehl J.F. 1986. Stratigraphy, paleomagnetism, and magnetic fabric of the Toba tuffs: constraints on the sources and eruptive style. *Journal of Volcanology and Geothermal Research* 56: 205–220.

Kraus S., Poblete F. and Arrigada C. 2010. Dike systems and their volcanic host rocks on King George Island, Antarctica: Implications on the geodynamic history based on multidisciplinary approach. *Tectonophysics* 495: 269–297.

LaBerge R., Porreca M. and Mattei M. 2009. Meandring flow of a pyroclastic density current documented by the anisotropy of magnetic susceptibility (AMS) in the quartz latite ignimbrite of the Pleistocene Monte Cimino volcanic centre (central Italy). *Tectonophysics* 446: 64–78.

Langroix F. and Banerjee S.K. 2004. The regional and temporal significance of primary aeolian magnetic fabrics preserved in Alaskan loess. *Earth and Planetary Science Letters* 225: 379–395.

MacDonald W.D. and Palmer H.C. 1990. Flow directions in ash-fow tufs: a comparison of geological and magnetic susceptibility measurements, Tshirege member (upper Bandelier Tuf), Valles Caldera, New Mexico, USA. *Bulletin of Volcanology* 53: 45–59, doi: 10. 1007/BF00680319.

Majdański M., Środa P., Malinowski M., Czuba W., Grad M., Guterch A. and Hegedűs E. 2008. 3D seismic model of the uppermost crust of the Admiralty Bay area, King George Island, West Antarctica. *Polish Polar Research* 29: 303–318.

Moncinhatto T.R., Haag M.B., Hartmann G.A., Savian J.F., Poletti W., Sommer C.A., Caselli A.T. and Trindade R.I. 2020. Mineralogical control on the magnetic anisotropy of lavas and ignimbrites: a case study in the Caviahue-Copahue field (Argentina). *Geophysical Journal International* 220: 821–838.

Nawrocki J., Pańczyk M. and Williams I.S. 2010. Isotopic ages and palaeomagnetism of selected magmatic rocks from King George Island (Antarctic Peninsula). *Journal of Geological Society, London* 167: 1063–1079.

Nawrocki J., Pańczyk M. and Williams I.S. 2011. Isotopic ages of selected magmatic rocks from King George Island (West Antarctica) controlled by magnetostratigraphy. *Geological Quarterly* 55: 301–322.

Nawrocki J., Pańczyk M., Wójcik K. and Kozłowska-Roman A. 2021. Age of volcanism on Keller Peninsula and assessment of age-constrained volcanic activity on King George Island, South Shetland Islands. *Polish Polar Research* 42: 77–95.

Pankhurst R.J. and Smellie J.L. 1983. K-Ar geochronology of the South Shetland Islands, Lesser Antarctica: apparent lateral migration of Jurassic to Quaternary island arc volcanism. *Earth Planetary Sciences Letters* 66: 214–222.

Pańczyk M. and Nawrocki J. 2011. Geochronology of selected andesitic lavas from the King George Bay area (SE King George Island). *Geological Quarterly* 55: 301–322.

Pańczyk M., Nawrocki J. and Williams I.S. 2009. Isotope age constraint for the Blue Dyke and Jardine Peak subvertical intrusions of King George Island, West Antarctica. *Polish Polar Research* 30: 379–391.

Rochette P., Aubourg C. and Perrin M. 1999. Is this magnetic fabric normal? A review and case studies in volcanic formations. *Tectonophysics* 307: 219–234.

Shi C., Zhu R. and Liu Q. 2003. Anisotropy of magnetic susceptibility of Hannuoba basalt, northern China: Constraints on the vent position of the lava sequences. *Geophysical Research Letters* 30: 1066, doi: 10.1029/2002GL016215.

Simón-Muzás A., Casas-Sainz A., Soto R., Gisbert J., Román-Berdiel T., Oliva-Urcia B., Pueyo E.L. and Beamud E. 2022. Axial longitudinal flow in volcanic materials of the Late Carboniferous-Permian Cadí basin (Southern Pyrenees) determined from anisotropy of magnetic susceptibility. *Journal of Volcanologu and Geothermal Research* 421: 107443, doi: 10.1016/j.jvolgeores.2021.107443.

Smellie J.L. 2021. Antarctic Peninsula – Geology and Dynamic Development. *In:* Kleinschmidt G. (Ed.) *Geology of the Antarctic continent*. Gebrüder Borntraeger Verlagsbuchhandlung, Stuttgart: 18–86.

Smellie J.L., Pankhurst R.J., Thomson M.R.A. and Davies R.E.S. 1984. The Geology of the South Shetland Islands: VI. Stratigraphy, Geochemistry and Evolution. *British Antarctic Survey Scientific Reports* 87: 1–85.

Smellie J.L., Hunt R.J., Mcintosh W.C. and Esser R.P. 2021a. Lithostratigraphy, age and distribution of Eocene volcanic sequences on eastern King George Island, South Shetland Islands, Antarctica. *Antarctic Science* 33: 373–401.

Smellie J.L., Mcintosh W.C., Whittle R., Troedson A. and Hunt R.J. 2021b. A lithostratigraphical and chronological study of Oligocene-Miocene sequences on eastern King George Island, South Shetland Islands (Antarctica), and correlation of glacial episodes with global isotope events. *Antarctic Science* 33: 502–532.

Tauxe L., Gee J.S. and Staudigel H. 1998. Flow directions in dikes from anisotropy of magnetic susceptibility data: the bootstrap way. *Journal of Geophysical Research* 103: 17,775–17,790.

Tokarski A.K. 1987. Structural events in the South Shetland Islands (Antarctica). IV. Structural evolution of King George Island and regional implications. *Studia Geologica Polonica* 93: 63–112.

Willan R.C.R. and Kelley S.P. 1999. Mafic dyke swarms in the South Shetland Islands volcanic arc: unraveling multi-episodic magmatism related to subduction and continental rifting. *Journal of Geophysical Research* 104: 23051–23068.

Zananiri I. and Kondopoulou D. 2004. Anisotropy of magnetic susceptibility (AMS) in volcanic formations: theory and preliminary results from recent volcanics of broader Aegean. *Bulletic of the Geological Society of Greece* 36: 1308–1315.